J|A|C|S ARTICLES

Published on Web 01/21/2009

Coumarin-Derived Cu^{2+}-Selective Fluorescence Sensor: Synthesis, Mechanisms, and Applications in Living Cells

Hyo Sung Jung,[†] Pil Seung Kwon,[‡] Jeong Won Lee,[†] Jae Il Kim,[†] Chang Seop Hong,[†] Jong Wan Kim,[‡] Shihai Yan,[§] Jin Yong Lee,*[,§] Jung Hwa Lee,[||] Taiha Joo,*[,||] and Jong Seung Kim*[,†]

Department of Chemistry, Korea University, Seoul 136-701, Korea, Department of Laboratory Medicine, Dankook University Hospital, Cheonan 330-715, Korea, Department of Chemistry, Institute of Basic Science, Sungkyunkwan University, Suwon 440-746, Korea, and Department of Chemistry, POSTECH, Pohang 790-784, Korea

Received November 3, 2008; E-mail: jinylee@skku.edu; thjoo@postech.ac.kr; jongskim@korea.ac.kr

Abstract: A novel coumarin-based fluorogenic probe bearing the 2-picolyl unit (**1**) was developed as a fluorescent chemosensor with high selectivity and suitable affinity in biological systems toward Cu^{2+} over other cations tested. The fluorescence on−off mechanism was studied by femtosecond time-resolved fluorescence (TRF) upconversion technique and ab initio calculations. The receptor can be applied to the monitoring of Cu^{2+} ion in aqueous solution with a pH span 4−10. To confirm the suitability of **1** for biological applications, we also employed it for the fluorescence detection of the changes of intracellular Cu^{2+} in cultured cells. The results indicate that **1** should be useful for the fluorescence microscopic imaging and the study on the biological functions of Cu^{2+}.

Introduction

A chemosensor is a compound that renders a significant change in electrical, electronic, magnetic, or optical signal when it binds to a specific guest counterpart. Of those sensors, fluorescent chemosensors have several advantages over the other methods due to their sensitivity, specificity, and real-time monitoring with fast response time.[1] In particular, for a certain purpose, it is highly demanding to selectively sense heavy metal ions such as mercury, lead, and copper.[2] The copper plays an important role in various biological processes.[3] However, exposure to a high level of copper even for a short period of time can cause gastrointestinal disturbance, while long-term exposure can cause liver or kidney damage.[4] The U.S. Environmental Protection Agency (EPA) has set the limit of copper in drinking water to be 1.3 ppm (∼20 μM). Also, the average concentration of blood copper in the normal group is 100−150 μg/dL (15.7−23.6 μM).[5]

In this connection, considerable efforts have been made to synthesize fluorescent chemosensors that are selective, sensitive, and suited to highly resolved imaging for monitoring biological processes.[6] Recently, many fluorescent chemosensors for Cu(II)-selective detection were reported and have been used with some success in biological applications.[7] However, some of them have shortcomings for practical application such as cross-sensitivities toward other metal cations, low water solubility, a narrow pH span, slow response, a low fluorescence quantum yield in aqueous media, and cytotoxicities of ligand.

Despite that a number of fluorescent chemosensors have been reported, the studies regarding detailed sensing mechanisms are scarce. To develop a new efficient chemosensor, a detailed sensing mechanism needs to be understood. Basically, fluorescence is a property of electronically excited states; thus, the

[†] Korea University.
[‡] Dankook University Hospital.
[§] Sungkyunkwan University.
[||] POSTECH.

(1) (a) Lai, C.-Y.; Trewyn, B. G.; Jeftinija, D. M.; Jeftinija, K.; Xu, S.; Jeftinija, S.; Lin, V. S.-Y. *J. Am. Chem. Soc.* **2003**, *125*, 4451. (b) Numata, M.; Li, C.; Bae, A.-H.; Kaneko, K.; Sakurai, K.; Shinkai, S. *Chem. Commun.* **2005**, 4655.
(2) (a) Rurack, K.; Kollmannsberger, M.; Resch-Genger, U.; Daub, J. *J. Am. Chem. Soc.* **2000**, *122*, 968. (b) Moon, S. Y.; Cha, N. R.; Kim, Y. H.; Chang, S.-K. *J. Org. Chem.* **2004**, *69*, 181.
(3) (a) Barceloux, D. G. *J. Toxicol.-Clin. Toxicol.* **1999**, *37*, 217. (b) Zhang, X. B.; Peng, J.; He, C. L.; Shen, G. L.; Yu, R. Q. *Anal. Chim. Acta* **2006**, *567*, 189. (c) Sarkar, B. In *Metal Ions in Biological Systems*; Siegel, H., Siegel, A., Eds.; Marcel Dekker: New York, 1981; Vol. 12, p 233. (d) Que, E. L.; Domaille, D. W.; Chang, C. J. *Chem. Rev.* **2008**, *108*, 1517.
(4) Georgopoulos, P. G.; Roy, A.; Yonone-Lioy, M. J.; Opiekun, R. E.; Lioy, P. J. *J. Toxicol. Environ. Health, B* **2001**, *4*, 341.
(5) Tak, W. T.; Yoon, S. C. *KSN* **2001**, *20*, 863.
(6) (a) Lee, J. W.; Jung, H. S.; Kwon, P. S.; Kim, J. W.; Bartsch, R. A.; Kim, Y.; Kim, S.-J.; Kim, J. S. *Org. Lett.* **2008**, *10*, 3801. (b) Kiyose, K.; Kojima, H.; Urano, Y.; Nagano, T. *J. Am. Chem. Soc.* **2006**, *128*, 6548. (c) Takakusa, H.; Kikuchi, K.; Urano, Y.; Sakamoto, S.; Yamaguchi, K.; Nagano, T. *J. Am. Chem. Soc.* **2002**, *124*, 1653. (d) Mello, J. V.; Finney, N. S. *J. Am. Chem. Soc.* **2005**, *127*, 10124. (e) Komatsu, K.; Urano, Y.; Kojima, H.; Nagano, T. *J. Am. Chem. Soc.* **2007**, *129*, 13447. (f) Miller, E. W.; Albers, A. E.; Pralle, A.; Isacoff, E. Y.; Chang, C. J. *J. Am. Chem. Soc.* **2005**, *127*, 16652.
(7) (a) Wu, Q.; Anslyn, E. V. *J. Am. Chem. Soc.* **2004**, *126*, 14682. (b) Xu, Z.; Qian, X.; Cui, J. *Org. Lett.* **2005**, *7*, 3029. (c) Weng, Y.-Q.; Yue, F.; Zhong, Y.-R.; Ye, B.-H. *Inorg. Chem.* **2007**, *46*, 7749. (d) Royzen, M.; Dai, Z.; Canary, J. W. *J. Am. Chem. Soc.* **2005**, *127*, 1612. (e) Zeng, L.; Miller, E. W.; Pralle, A.; Isacoff, E. Y.; Chang, C. J. *J. Am. Chem. Soc.* **2006**, *128*, 10. (f) Shao, N.; Zhang, Y.; Cheung, S.; Yang, R.; Chan, W.; Mo, T.; Li, K.; Liu, F. *Anal. Chem.* **2005**, *77*, 7294. (g) Yang, L.; McRae, R.; Henary, M. M.; Patel, R.; Lai, B.; Vogt, S.; Fahrni, C. J. *Proc. Natl. Acad. Sci. U.S.A.* **2005**, *102*, 11179. (h) Kramer, R. *Angew. Chem.* **1998**, *110*, 804. (i) Zhang, X.; Shiraishi, Y.; Hirai, T. *Org. Lett.* **2007**, *9*, 5039. (j) Xu, Z.; Xiao, Y.; Qian, X.; Cui, J.; Cui, D. *Org. Lett.* **2005**, *7*, 889.

 10.1021/ja808611d CCC: $40.75

Scheme 1. Synthetic Pathways to **1**−**3**

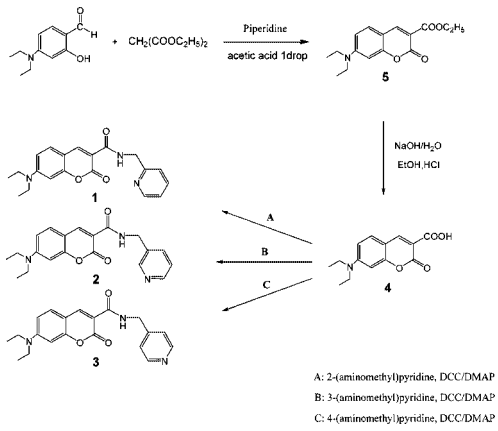

Scheme 2

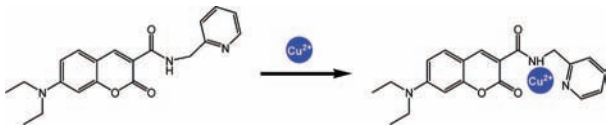

mechanism can be understood by time-resolved laser spectroscopy based on quantum mechanics. Previously, the quantum calculations have given successful understanding for the experimentally observed fluorescence behaviors of several chemosensors.[8] However, the calculation results do not give any information on the lifetime of the fluorescence decay, which is a key factor for the mechanism. Furthermore, it is hardly understood by calculations if the fluorescence quenching mainly arises from charge transfer or energy transfer. For more accurate understanding of the fluorescence mechanism, state-of-the-art time-resolved femtosecond laser spectroscopic study is highly demanding as well as the quantum calculations.

Here, we synthesized a new coumarin-derived Cu(II)-selective fluorescent sensor (**1**) and studied the fluorescence quenching mechanism by femtosecond time-resolved fluorescence spectroscopy and quantum calculations. We also herewith present the bioapplication of **1** to monitor Cu(II) in cultured cells.

Results and Discussion

Compounds **1**−**3** were synthesized in 60%, 64%, and 57% yields via a three-step procedure, respectively (Scheme 1). As depicted in Scheme 1, to envision the binding mode of the picolyl unit, 2−4-picolyl substrates were introduced to coumarin amide unit. The structures of **1**−**3** were confirmed by ^{1}H NMR, ^{13}C NMR, FT-IR, and FAB-MS (Figures S12−S21). The binding mode of **1**−Cu^{2+} is illustrated in Scheme 2.

The single crystal of **1**−Cu^{2+} was grown by mixing equivalent **1** and $Cu(ClO_4)_2$ under vapor diffusion of EtOH into a solution of CH_3CN and water. The crystal structure of **1**−Cu^{2+} is shown in Figure 1, representing 1:1 stoichiometry between **1** and Cu^{2+}. The Cu^{2+} ion binds a coumarin O_3 atom, a coumarin amide N_2 atom, a pyridine N_1 atom, and two oxygen O_4, O_5 atoms of water. More detailed data are provided in the supporting CIF data.

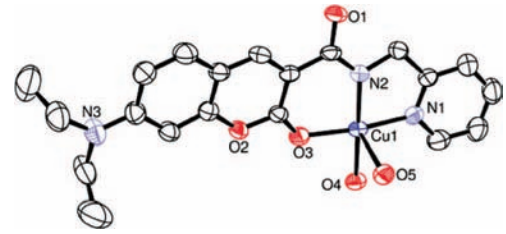

Figure 1. Crystal structure of **1**−Cu^{2+}. All hydrogen atoms are omitted for clarity.

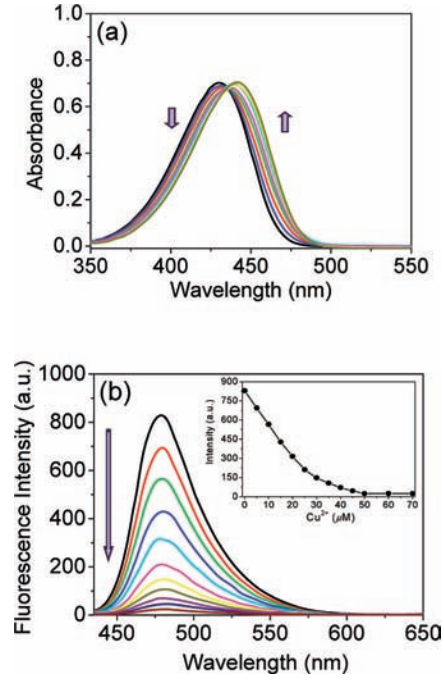

Figure 2. (a) Absorption spectra and (b) fluorescence spectra of **1** (20 and 5 μM, respectively) with addition of various concentrations of $CuCl_2$ [0, 5, 10, 15, 20, 25, 30, 35, 40, 45, and 50 μM, respectively] in aqueous solution (HEPES:DMSO = 9:1, v/v) (0.01 M) with an excitation at 430 nm.

Figure 2 shows changes of absorption and fluorescence spectra of the aqueous solution (HEPES:DMSO = 9:1, v/v) of **1** upon addition of Cu^{2+}. Addition of 10 equiv of Cu(II) produced a 15 nm red shift of the absorption maximum, resulting in a perceived color change from yellow to dark yellow, while the fluorescence was almost quenched in stark contrast to other metal cations, where no significant fluorescence changes were observed. Even with highly concentrated Na^{2+}, K^+, Ca^{2+}, and Mg^{2+} (~5.0 mM) under physiological conditions,[9] we found no fluorescence changes in **1**. By measuring the emission maximum of **1**−Cu^{2+}, the fluorescence change of **1** responds to the range of 0−50 μM of [Cu^{2+}]. We then found that **1** shows 0.5 μM of detection limit able to sufficiently sense the Cu^{2+} concentration in the blood system. Moreover, the detection limit is to be satisfactory to the Cu^{2+} detection in drinking water within U.S. EPA limit (~20 μM). Using the fluorescence titration data, the binding constant of **1** with Cu^{2+} in aqueous solution was found to be $(1.17 \pm 0.29) \times 10^5$. The detailed fluorescence changes are shown in Figure S1.

(8) (a) Cho, E. J.; Moon, J. W.; Ko, S. W.; Lee, J. Y.; Kim, S. K.; Yoon, J.; Nam, K. C. *J. Am. Chem. Soc.* **2003**, *125*, 12376. (b) Lee, J. Y.; Cho, E. J.; Mukamel, S.; Nam, K. C. *J. Org. Chem.* **2004**, *69*, 943. (c) Kim, S. K.; Lee, S. H.; Lee, J. Y.; Lee, J. Y.; Bartsch, R. A.; Kim, J. S. *J. Am. Chem. Soc.* **2004**, *126*, 16499. (d) Kim, S. K.; Bok, J. H.; Bartsch, R. A.; Lee, J. Y.; Kim, J. S. *Org. Lett.* **2005**, *7*, 4839. (e) Ryu, D.; Park, E.; Kim, D.-S.; Yan, S.; Lee, J. Y.; Chang, B.-Y.; Ahn, K. H. *J. Am. Chem. Soc.* **2008**, *130*, 2394.

(9) Rae, T. D.; Schmidt, P. J.; Pufahl, R. A.; Culotta, V. C.; O'Halloran, T. V. *Science* **1999**, *284*, 805.

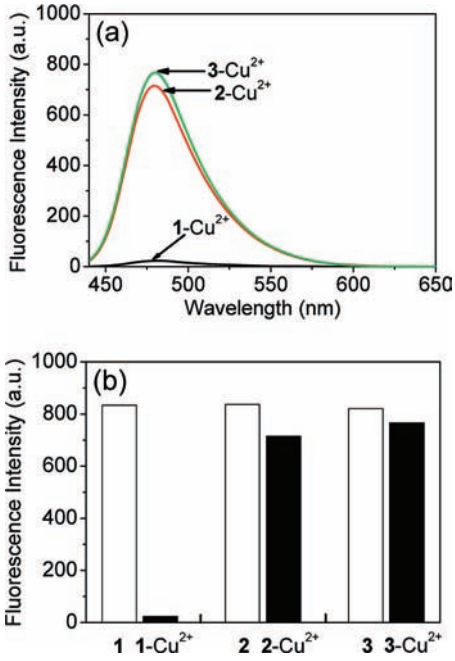

Figure 3. (a) Fluorescence spectra of **1**−**3** (5 μM, respectively) with addition of $CuCl_2$ (10 equiv, respectively) in aqueous solution (HEPES:DMSO = 9:1, v/v) (0.01 M) with an excitation at 430 nm. (b) Relative responses at 479 nm of **1**−**3** (5 μM, respectively) (white bars) and **1**−**3** (5 μM, respectively) with addition of $CuCl_2$ (10 equiv, respectively) (black bars) in aqueous solution (HEPES:DMSO = 9:1, v/v) (0.01 M) with an excitation at 430 nm.

To understand a crucial role of 2-picolyl unit, which behaves as an additional binding site for the Cu^{2+} ion with an aid of the coumarin amide, we have synthesized **2** and **3** bearing 3-picolyl and 4-picolyl units on the coumarin amide, respectively. Subsequently, they were tested for fluorescence changes upon the addition of copper ion as well. As seen in Figure 3, unlike **1**, neither of them shows any distinct absorption or fluorescence spectral changes upon addition of Cu^{2+} ion. This strongly supports that the 2-position of the nitrogen atom in the pyridine group plays an important role for the Cu^{2+} complexation in a three-dimensional way. In the presence of 10 equiv of Cu^{2+} ion, the fluorescence difference between **1** and **1**−Cu^{2+} is ∼50 times greater than that between **2** and **2**−Cu^{2+}. We also found a remarkable selectivity of **1** for Cu^{2+} ion over various other metal ions in single and multicomponent systems, which turned out to be applicable in environmental technology (Figure S4).

It is well-known that heavy metal ions such as Cu^{2+}, Cd^{2+}, Hg^{2+}, and Pb^{2+} tend to quench the luminescence through electron- and/or energy-transfer processes.[10] To get an insight into the quenching behavior in the **1**−Cu^{2+} complex, we have measured femtosecond time-resolved fluorescence (TRF) by the fluorescence upconversion technique. The fluorescence decay behavior in the presence of Cu^{2+} is shown in Figure 4, and the exponential fit results are summarized in Table 1.

In the absence of Cu^{2+}, the fluorescence decays single exponentially by 93 ps time constant, which is the lifetime of the S_1 state of free **1**. As Cu^{2+} is added to the solution, an ultrafast component in the range of 150−190 fs emerges to result

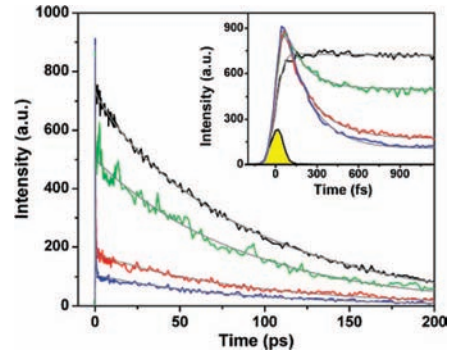

Figure 4. Time-resolved fluorescence of **1** with an excitation at 430 nm in the absence (black) and in the presence of 1 equiv (green), 2 equiv (red), and 3 equiv (blue) of Cu^{2+} ions. Inset shows the decay in short time region. The yellow peak indicates instrumental response measured by the solvent Raman signal.

Table 1. Fluorescence Decay Time Constants of **1** in the Presence of Cu^{2+} Ions

Cu^{2+} (equiv)	A_1	τ_1 (fs)	A_2	τ_2 (ps)
0			100%	93
1	55%	150	44%	86
2	85%	190	15%	90
3	92%	190	8%	82

in a biexponential fluorescence decay. As the amount of Cu^{2+} increases, the fast decay component increases (55%, 85%, and 92% for 1, 2, and 3 equiv of Cu^{2+}, respectively), while the slow decay component decreases accordingly. Upon addition of 3 equiv of Cu^{2+}, the TRF of **1** decays mostly by 190 fs time constant to show that **1** is quenched efficiently by ligation with Cu^{2+}. More importantly, the time constant (τ_2) of the lifetime decay component is mostly constant while Cu^{2+} is added. Invariance of τ_2 clearly indicates that the fluorescence spectra consist of two contributions, one from free **1** (τ_2) and the other from **1**−Cu^{2+} (τ_1), although the stationary fluorescence spectra do not change upon addition of Cu^{2+}. Thus, the ultrafast decay must be related to the interaction between **1** and Cu^{2+}. On the basis of the relative amplitudes of the two decay components, the binding constant between **1** and Cu^{2+} is calculated to be 4.4×10^4, which is in good agreement with the stationary result and corroborates our assignment. Because the fluorescence spectrum does not change upon addition of Cu^{2+}, one can rule out the possibility of forming a charge-transfer emitting state within **1**. Instead, the interaction between **1** and Cu^{2+} provides an additional fluorescence quenching pathway. The fluorescence quenching of the ligand may occur by the excitation energy transfer from the ligand to the metal d-orbital and/or ligand to metal charge transfer (LMCT).[11]

To elaborate upon the mechanism of the fluorescence quenching by the energy and/or charge transfer model, we carried out the ab initio calculations (Figure 5; details in Figure S7). From this calculation, we noticed that the fluorescence quenching by Cu^{2+} could be rationalized in terms of the occupancy of the frontier orbitals. The HOMO → LUMO+4 and HOMO → LUMO+6 excitations were found to be relevant to the LMCT, and their contributions to the lowest energy excitation were 18% and 11%, respectively. These excitations

(10) (a) Kavallieratos, K.; Rosenberg, J. M.; Chen, W.-Z.; Ren, T. *J. Am. Chem. Soc.* **2005**, *127*, 6514. (b) Zheng, Y.; Orbulescu, J.; Ji, X.; Andreopoulos, F. M.; Pham, S. M.; Leblanc, R. M. *J. Am. Chem. Soc.* **2003**, *125*, 2680. (c) Quang, D. T.; Jung, H. S.; Yoon, J. H.; Lee, S. Y.; Kim, J. S. *Bull. Korean Chem. Soc.* **2007**, *28*, 682.

(11) (a) Ressalan, S.; Iyer, C. S. P. *J. Lumin.* **2005**, *111*, 121. (b) Choi, M.-Y.; Chan, M. C.-W.; Zhang, S.; Cheung, K.-K.; Che, C.-M.; Wong, K.-Y. *Organometallics* **1999**, *18*, 2074. (c) Villata, L. S.; Wolcan, E.; Feliz, M. R.; Capparelli, A. L. *J. Phys. Chem. A* **1999**, *103*, 5661.

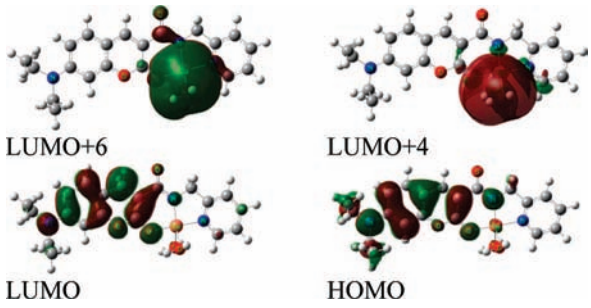

Figure 5. Frontier molecular orbitals of **1**−Cu^{2+} relevant to the fluorescence quenching.

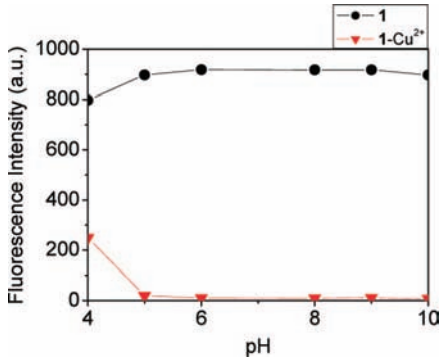

Figure 6. Variation of fluorescence spectra of **1** (5 μM) in aqueous solution (HEPES:DMSO = 9:1, v/v) (0.01 M) with and without Cu^{2+} (10 equiv) ion as a function of pH. Fluorescence intensity (au) at 479 nm.

correspond to charge transfer from the excited coumarin moiety to the Cu^{2+} center (LMCT) and thus provide a pathway for nonradiative deactivation of the excited state. Based on the calculations, LMCT contribution is about 29%. Thus, considering the TRF experimental results, the energy transfer may also significantly contribute to the nonradiative deactivation of the excited state.

For the biological application of the fluorescent sensor, the sensing should operate in a wide range of pH. Figure 6 shows that in aqueous solution the suitable pH range for Cu^{2+} determination is pH 4−10 where the florescence "on−off" can be operated by the copper ion binding. Consequently, our present Cu^{2+}-selective receptor would be an ideal fluorometric chemosensor for monitoring Cu^{2+}.

The ability of biosensing molecules to selectively monitor guest species in living cells is of great importance for biological application.[12] Considering that copper accumulation leads to toxicity in animals, we primarily carried out experiment using **1** on liver and kidney cell lines in which Cu^{2+} is known to be accumulated. LLC-MK2 cells (kidney cells of monkey) were cultured in Dulbecco's modified Eagle's medium (DMEM), supplemented with 10% (v/v) heat-inactivated fetal calf serum (HyClone), 100 μg/mL penicillin, 100 μg/mL streptomycin, and 0.25 mM L-glutamine, at 37 °C in 5.0% CO_2 humidified air for 7 days. First, to determine the cell permeability of **1**, LLC-MK2 cells were incubated with **1** (5 μM) for 10−20 min at 37 °C, and washed with PBS to remove the remaining compound **1**. The results are shown in Figure 7b and Figure S11. One can clearly observe significant confocal imaging changes of the

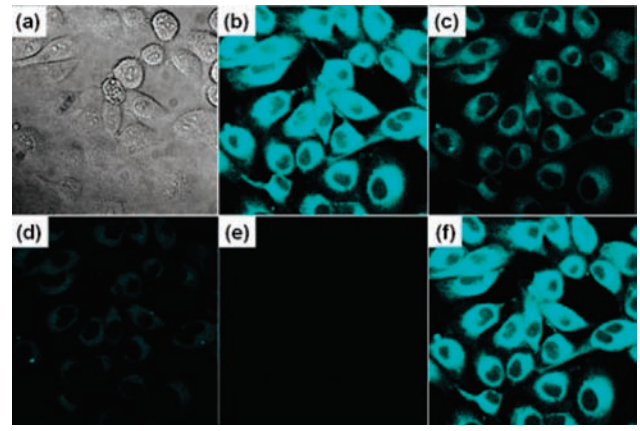

Figure 7. Confocal fluorescence images of Cu^{2+} in LLC-MK2 cells (Zeiss LSM 510 META confocal microscope, 40× objective lens). (a) Bright-field transmission image of LLC-MK2 cells. (b) Fluorescence image of LLC-MK2 cells incubated with **1** (5 μM). Further incubated with addition of various concentrations of $CuCl_2$ [(c) 5, (d) 10, and (e) 20 equiv, respectively]. (f) Return of intracellular Cu^{2+} to the resting level was achieved by addition of EDTA (500 μM).

medium upon addition of $CuCl_2$ for 20 min (5, 10, and 20 equiv, respectively) at 37 °C. LLC-MK2 cells incubated with **1** initially display a strong fluorescent image, but the fluorescence image immediately becomes faint in the presence of Cu^{2+} (Figure 7c−e). Lowering the concentration of **1** down to 1.0 μM, we also can obtain the confocal image changes (Figure S10).

In addition, for further biological application point of view, we then employed MTT assay to investigate cytotoxicity of **1** and [Cu^{2+}] to the cell lines (Figures S8).[13] The cell viability declines by 50−70% upon Cu^{2+} (~23.6 μM) treatment, while the viability of the copper-poisoned cell increases to 40% by the addition of **1**. Therefore, it should be noteworthy that **1** is effective for enhancing cell viability, which was diminished by Cu^{2+}. Thus, **1** can be a suitable fluorescence chemosensing probe for Cu^{2+} detection in biological systems.

Conclusions

Coumarin derivative **1** appending 2-picolylamide enables efficient tridentate complextion for Cu(II) in preference to a variety of other common heavy and toxic metal ions. Complexation mode and the corresponding quenching mechanism were elucidated by the femtosecond time-resolved fluorescence upconversion technique and ab initio calculations. In a sense of water solubility, membrane permeability, and nontoxic nature, **1** could be one of the most important sensing probes for the detection of Cu(II) in living cells.

Experimental Section

Synthesis. 4 and **5** were synthesized according to the reported procedures.[14]

7-(Diethylamino)-2-oxo-*N*-((pyridin-2-yl)methyl)-2H-chromene-3-carboxamide (1). To a vigorously stirred suspension of **4** (2.34 g, 10 mmol) in chloroform (100 mL) were added dicyclohexylcarbodiimide (DCC) (2.3 g, 11 mmol), 2-(aminomethyl)pyridine (1.32 g, 11 mmol), and a catalytic amount of 4-(dimethylamino)pyridine (DMAP) (50 mg). The mixture was stirred for 6 h, and the white precipitate *N*,*N*′-dicyclohexylurea (DCU) was filtered from the yellow solution. The filtrate was washed with water (3 × 50

(12) (a) Chang, M. C. Y.; Pralle, A.; Isacoff, E. Y.; Chang, C. J. *J. Am. Chem. Soc.* **2004**, *126*, 15392. (b) Peng, X.; Du, J.; Fan, J.; Wang, J.; Wu, Y.; Zhao, J.; Sun, S.; Xu, T. *J. Am. Chem. Soc.* **2007**, *129*, 1500.

(13) Rooney, J. P. K. *Toxicology* **2007**, *234*, 145.

(14) Ma, Y.; Luo, W.; Quinn, P. J.; Liu, Z.; Hider, R. C. *J. Med. Chem.* **2004**, *47*, 6349.

mL) and dried over anhydrous sodium sulfate, and the solvent was removed in vacuo. The crude product was further purified by column chromatography on alumina B-10 (eluant: ethyl acetate: dichloromethane, 1:5 v/v) to afford a yellow solid (2.12 g, 60%): mp 170 °C. ^{1}H NMR (200 MHz, $CDCl_3$): δ 1.21−1.28 (m, 6H), 3.44−3.48 (m, 4H), 4.80 (d, 2H), 6.5 (d, 1H), 6.65 (d, 1H), 7.18 (m, 1H), 7.30 (m, 1H), 7.43 (m, 1H), 7.65 (m, 1H), 8.60 (d, 1H), 8.74 (s, 1H), 9.53 (s, 1H). ^{13}C NMR (50 MHz, $CDCl_3$): δ 12.42, 28.76, 45.07, 45.32, 96.66, 100.00, 108.41, 109.92, 110.33, 121.57, 122.09, 128.20, 131.14, 136.64, 148.24, 149.37, 152.59, 157.68, 157.74, 163.40. FAB-MS calcd for $C_{20}H_{21}N_3O_3$ $[M + H]^+$ 351.41, found 351.00.

Analogous procedures starting with coumarin acids with amino derivatives gave **2** and **3**.

7-(Diethylamino)-2-oxo-*N*-((pyridin-3-yl)methyl)-2H-chromene-3-carboxamide (2). (2.24 g, 64%): mp 190−192 °C. ^{1}H NMR (200 MHz, $CDCl_3$): δ 1.21−1.28 (m, 6H), 3.44−3.48 (m, 4H), 4.80 (d, 2H), 6.5 (d, 1H), 6.65 (d, 1H), 7.25 (m, 1H), 7.42 (d, 1H), 7.72 (d, 1H), 8.51 (d, 1H), 8.61 (s, 1H), 8.74 (s, 1H), 9.23 (s, 1H). ^{13}C NMR (50 MHz, $CDCl_3$): δ 12.42, 34.12, 45.07, 96.48, 108.28, 109.62, 110.00, 123.46, 128.14, 131.19, 134.17, 135.38, 148.41, 148.63, 149.22, 152.65, 157.67, 162.75, 163.45, 177.86. FAB-MS calcd for $C_{20}H_{21}N_3O_3$ $[M + H]^+$ 351.41, found 351.00.

7-(Diethylamino)-2-oxo-*N*-((pyridin-4-yl)methyl)-2H-chromene-3-carboxamide (3). (2.00 g, 57%): mp 210−212 °C. ^{1}H NMR (200 MHz, $CDCl_3$): δ 1.21−1.28 (m, 6H), 3.44−3.48 (m, 4H), 4.68 (d, 2H), 6.53 (d, 1H), 6.68 (d, 1H), 7.19 (m, 1H), 7.35 (d, 1H), 7.43 (d, 1H), 8.56 (d, 2H), 8.74 (s, 1H), 9.30 (s, 1H). ^{13}C NMR (50 MHz, $CDCl_3$): δ 12.38, 33.93, 45.10, 96.53, 108.32, 109.52, 110.08, 122.20, 122.21, 131.27, 139.95, 147.63, 148.56, 148.56, 149.96, 149.97, 152.74, 157.74, 162.87, 163.63. FAB-MS calcd for $C_{20}H_{21}N_3O_3$ $[M + H]^+$ 351.41, found 351.01.

DFT Calculations. Density functional theory (DFT) calculations with Becke's three parametrized Lee−Yang−Par (B3LYP) exchange functionals with 6-31G* basis sets were carried out for the geometry optimizations of **1** and **1**−Cu^{2+} complex using a suite of Gaussian 03 programs. The time-dependent DFT (TDDFT) calculations were performed to have the excitation energies and oscillator strengths at the optimized geometries.

Time-Resolved Spectroscopy. Time-resolved fluorescence was measured by noncollinear fluorescence upconversion technique described elsewhere.[15] Light source was a home-built cavity dumped Ti:sapphire oscillator pumped by a frequency doubled Nd:YVO_4 laser (Verdi, Coherent Inc.). The center wavelength of the oscillator output was 830 nm. Pump pulses at 415 nm were generated by the second harmonic generation in a 200 μm thick lithium-triborate (LBO) crystal. The energy of pump pulse was about 4 nJ at 380 kHz. The time resolution was 100 fs for the 500 μm thick β-barium borate (BBO) mixing crystal. The sample concentration was set to 100 μM to give absorbance of 0.1 in a 200 μm cuvette.

Absorption and Fluorescence Spectra. Stock solutions (1.00 mM) of the metal chloride salts were prepared in water. Stock solutions of **1** (0.3 mM) were prepared in H_2O/DMSO solution (9/1, v/v). For all measurements of fluorescence spectra, excitation was at 430 nm with excitation and emission slit widths at 3.0 nm. UV/vis and fluorescence titration experiments were performed using 20 and 5 μM of **1** in H_2O/DMSO solution (9/1, v/v) with varying concentrations of the metal chloride salts. After the concentrations of the free ligands and complexed forms of **1** and **2** were calculated from the fluorescence titration experiments, the association constants were obtained using the computer program ENZFITTER.[16]

Cell Incubation. Two cell lines (LLC-MK2, and NCTC clone 1469 cells, respectively) for fluorescence imagines were used. Cell lines were prepared from continuous culture in Dulbeccos modified Eagles medium (GibcoBRL, USA), supplemented with 10% (v/v) heat-inactivated fetal calf serum (HyClone), 100 μg/mL penicillin, 100 μg/mL streptomycin, and 0.25 mM L-glutamine, at 37 °C in 5.0% CO_2 humidified air. When the cells reached the logarithmic phase, the cell density was adjusted to 1.0×10^5 per/well in culture media. The cells were then used to inoculate in a glass bottom dish, with 1.0 mL of cell suspension in each dish. After cell adhesion, culture medium was removed. The cell layer was rinsed twice with phosphate buffered saline (PBS), and then 1.0 mL of culture medium was added in each dish.

Confocal Fluorescence Images with Intracellular-Cu^{2+}. To determine the cell permeability of Cu^{2+}, all cell lines were incubated with **1** (5 μM) for 1 day at room temperature. Upon addition of 5 equiv of Cu^{2+} into the cell line, the fluorescence image of intracellular Cu^{2+} was observed under a Zeiss LSM 510 META confocal microscope. Excitation wavelength of laser was 405 nm, and emission spectra were integrated over the range 450−520 nm (single channel). For all images, the confocal microscope settings, such as transmission density, brightness, contrast, and scan speed, were held constant to compare the relative intensity of intracellular Cu^{2+} fluorescence.

MTT Assay. LLC-MK2 cell lines were inoculated into a 96-well, flat-bottomed microplate (Nunc, DNK) at a volume of 100 μL (5 × 104 cells/mL) for a stationary culture. The media were exchanged into new fresh media. The cells were treated in the 2-fold down dilution series of **1** (50 μM), Cu^{2+} (50 μM), and **1** (50 μM) plus each well into Cu^{2+} (50 μM) and then incubation in the 5% CO_2 at 37 °C, for 1 day. Cells were added to MTT [3-(4,5-dimethylthiazol-2-yl)-2,5-diphenyltetrazolium bromide] solution (2 mg/mL, Sigma). After an incubation in 5% CO_2 at 37 °C, for 4 h, the solution was changed into 150 μL of dimethysulfoxide (DMSO: Kanto, Japan) and shaken in a microplate mixer (Amersham, UK) for 10 min. The optimal density (OD) value was measured by a microplate reader (BIO-RAD 550, CA) using 540 nm wavelength. The cell viability was calculated by the following formula: (mean OD in treated wells ÷ mean OD in control wells) × 100.

Acknowledgment. This work is supported by the KOSEF Grant funded by MOST (R11-2007-012-03002-0) (2008) and SRC (R11-2005-008-02001-0(2008)).

Supporting Information Available: Synthetic details, additional NMR, UV, and emission spectral data, MTT assay, and pH span. This material is available free of charge via the Internet at http://pubs.acs.org.

JA808611D

(15) Rhee, H.; Joo, T. *Opt. Lett.* **2005**, *30*, 96.

(16) (a) Association constants were obtained using the computer program ENZFITTER, available from Elsevier-BIOSOFT, 68 Hills Road, Cambridge CB2 1LA, UK. (b) Connors, K. A. *Binding Constants*; Wiley: New York, 1987.